
ORIGINAL ARTICLE

Regional Variation within the Cerebral Cortex Evaluated by Diffusion-weighted Imaging and Apparent Diffusion Coefficients on 1.5T and 3T Magnetic Resonance Images

TW Yeung, HY Lau, YC Wong

Department of Radiology, Tuen Mun Hospital, Tuen Mun, Hong Kong

ABSTRACT

Objectives: We aimed to determine whether cerebral cortices have regional variation on diffusion-weighted magnetic resonance imaging (DW-MRI) and corresponding apparent diffusion coefficient (ADC) maps. We also aimed to explore the effect of using 1.5T and 3T MRI with respect to such regional variation.

Methods: Axial 5 mm-thick DW-MR images at 1.5T and 3T of 49 neurologically normal adults (24 men and 25 women; mean age, 44 years; age range, 21-76 years) were evaluated retrospectively. The cortical signal intensities (SIs) at the frontal, parietal, occipital, and temporal lobes, as well as the cingulate gyri, insula, hippocampus, and amygdala were qualitatively categorised into five grades, relative to that of the right frontal lobe. Contrast ratios (CRs) on DW-MR images were compared for each area. ADC values for corresponding regions were also measured to analyse the diffusion change. With respect to male and female subjects and left and right hemispheres, CR difference and ADC values in each cortex were tested using one-way analysis of variance (ANOVA) for multiple comparisons. Once statistically significant differences were identified, post-hoc analysis by Tukey's range test was performed. All statistical levels of significance were set at 5%. Results for patients imaged by 1.5T (n = 25) and 3T (n = 24) MRI machines were compared.

Results: Increased SI was demonstrated in the cingulate gyri and insula regardless of patient age, gender, or laterality-related difference. The visual grading of SI in the cingulate gyri and insula was higher than that of right frontal cortex in most subjects, more pronounced in 3T (cingulate: 100%; insula: 96%) than 1.5T (cingulate: 96%; insula: 82%) MRIs. ANOVA showed statistically significant differences among the means of various groups in both 3T and 1.5T groups of these subjects. The CRs measured at the cingulate gyrus and insula on both sides were significantly higher than that of other cortical areas in 3T MRI ($p < 0.05$). Although higher SIs at the cingulate gyri and insulae were found on visual grading, no consistent significant CR heterogeneity was demonstrated at these regions in 1.5T MRI. There was no significant apparent ADC difference on quantitative evaluation of the values at various cortices, indicating that the regional heterogeneity on DWI was caused by a T2 shine-through effect.

Conclusion: On DWI, high SIs at the cingulate gyri and insular cortices are frequently observed in neurologically normal adults. Absence of ADC map differences signifies that these findings are not related to restricted diffusion, but are caused by T2 shine-through effect. This reflects the basic cytoarchitectural difference between allocortex and periallocortex with the neocortex, as documented in previous literature. 3T MRI accentuates the depiction of physiological cortical heterogeneity on DWI. Awareness of normal patterns and special consideration of the variations of cortical appearance on DWI are necessary when evaluating cortex pathology, especially with the use of high-field MRI.

Key Words: Brain mapping; Cerebral cortex; Diffusion magnetic resonance imaging

Correspondence: Dr Tsz-wai Yeung, Department of Radiology, Tuen Mun Hospital, Tuen Mun, Hong Kong.
Tel: (852) 2468 5177; Fax: (852) 2466 3569; Email: kaylayeung@gmail.com

Submitted: 25 Feb 2013; Accepted: 3 Apr 2013.

中文摘要

應用1.5T和3T磁共振彌散加權成像和表觀彌散系數評估大腦皮層區域差異

楊子慧、劉顯宇、王耀忠

目的：確定大腦皮層在彌散加權磁共振成像（DW-MRI）和相應的表觀彌散系數（ADC）圖中是否有區域差異，並探討使用1.5T和3T磁共振對此區域差異的影響。

方法：研究對象為49名神經功能正常的成年人（24男和25女；平均年齡44歲，介乎21至76歲），評估他們軸向5毫米層厚的DW-MRI（1.5T和3T）圖像。以大腦右前額葉信號強度為參照標準，將額葉、頂葉、枕葉、顳葉，以及扣帶回、腦島、海馬和杏仁核的皮層信號強度定性地分為5個等級。把每個區域DW-MRI的對比度（CRs）進行了比較，並測量相應區域的ADC值來分析彌散變化。運用單因素方差分析（ANOVA），多重比較男性與女性之間，左右半球之間各個皮層區的對比度差異及ADC值。一旦達至統計學上的意義便以Tukey's差距檢定的方法進行事後分析。統計顯著性水平設定為5%。再比較分別用1.5T（n = 25）和3T（n = 24）MRI掃描得出的兩組數據。

結果：扣帶回和腦島皮層信號強度增強，且無年齡、性別或偏側差異。在大部份的參與者中，扣帶回和腦島的目測信號強度高於右額葉皮層，並且3T（扣帶回：100%；腦島：96%）比1.5T（扣帶回：96%；腦島：82%）的磁共振成像更明顯。ANOVA測試顯示這些研究對象中不同組別平均值有顯著統計學差異，1.5T及3T磁共振成像均是如此。3T MRI中，雙側大腦半球扣帶回和腦島的CRs均顯著高於其他皮層區（ $p < 0.05$ ）。雖然發現扣帶回和腦島的目測信號強度較高，可是1.5T MRI中這些皮層區並無對應的CR顯著差異。在對不同皮層區ADC值定量分析，結果並無顯著差異；提示DWI上皮層信號的區域差異是由T2穿透效應導致。

結論：神經功能正常的成年人的DWI圖像上，扣帶回和腦島皮質高信號強度很常見。但其ADC圖上並無差異，提示該現象與彌散受限無關，而是由T2穿透效應導致。這反映了舊皮層、周圍舊皮層、以及新皮層之間基本細胞結構的差異，如以往文獻所述。DWI圖像顯示了腦皮層的生理差異，這點於3T MRI中尤為突出。評估腦皮層病理變化時，必須注意DWI圖像上腦皮層信號的正常表現，特別考慮皮層信號的區域差異；尤其是使用高場強MRI時。

INTRODUCTION

Diffusion-weighted magnetic resonance imaging (DW-MRI) has become increasingly used and recognised as a powerful neuroimaging tool for the diagnosis of a wide range of pathology. Predominantly cortical diffusion abnormalities have been reported for various diseases, including acute ischaemic infarcts,¹⁻³ Creutzfeldt-Jakob disease (CJD),⁴ herpes simplex encephalitis,^{5,6} post-ictal status,⁷⁻⁹ and reversible posterior leukoencephalopathy syndrome.¹⁰

High signal intensities (SIs) at the cingulate gyri and insular cortices are frequently encountered on DW images of neurologically healthy adults, more obvious

when studied with 3T MRI as compared with 1.5T. Hence it is necessary to have reference standards for normal or physiologically high-signal cerebral cortices, to avoid misdiagnosis.

Regional variation in cellular morphology, cytoarchitecture, water content, diffusivity, iron concentration, microcirculation, and metabolic activity of human brain cortex have been documented by using histological, physiological, and imaging studies.¹¹⁻¹⁴ Heterogeneity in cortical SI on T2-weighted fast spin-echo and fast fluid-attenuated inversion recovery (FLAIR) MR images have also been described.^{15,16} However, to date, only a few reports¹⁷⁻¹⁹ looking at

cortical signal heterogeneity on DW-MRI have been available, and none has investigated the apparent diffusion coefficient (ADC) value and the effect of cortical signal variations by using high-strength MRI machines. The purpose of our study was to determine whether the brain cortices have different SIs on DW-MRI. We also looked into the effect of using 3T and 1.5T MRI on such regional variation.

METHODS

Patient Population

A consecutive series of patients referred for routine MRI of the brain from January 2011 to June 2011 were retrospectively reviewed. The MR images were reviewed in consensus by two radiologists to exclude any focal lesion. We excluded patients with a history of neurological disease, malignancy, stroke, or brain surgery. A total of 49 patients (24 men and 25 women) with a mean age of 44 (range, 21-76) years were recruited. The distribution of the patients by age and gender is shown in Table 1. Indications of MRI included headache (n = 30), dizziness (n = 11), psychiatric problems (n = 2), paresthesia (n = 2), tinnitus (n = 2), amnesia (n = 1), and tremor (n = 1).

Imaging Procedures

In all, 25 MRIs were obtained with a 1.5T system (Philips Achieva 1.5T; Philips, The Netherlands), while there were 24 images with a 3T system (Philips Achieva 3.0T Tx; Philips, The Netherlands) equipped with a circularly polarised head coil.

For DW images, whole-brain axial plane, single-shot spin-echo planar imaging was acquired by applying diffusion-sensitising gradients along three orthogonal directions, with a diffusion weighting factor $b = 1000 \text{ s/mm}^2$ plus one reference scan with $b = 0$.

Table 1. Distribution of patients according to age and sex.

Patient age (years)	No. of patients imaged using 1.5T MRI* (n = 25)	No. of patients imaged using 3T MRI* (n = 24)
18-30	5 (2/3)	4 (0/4)
31-40	3 (0/3)	5 (3/2)
41-50	4 (2/2)	8 (5/3)
51-60	9 (5/4)	6 (3/3)
61-70	3 (3/0)	1 (0/1)
71-80	1 (1/0)	0
Total	25 (13/12)	24 (11/13)
Mean age (years)	42.3	45.9

Abbreviation: MRI = magnetic resonance imaging.

* Numbers in parentheses are the number of male/female subjects.

Moreover, 3T- and 1.5T-weighted scan parameters were TR/TE 2800/88 ms and 3000/65 ms, respectively. The field of view was 230 x 230 mm²; the matrix size was 128 x 128; the section thickness was 5 mm; and the section gap was 1 mm. Sensitivity encoding (SENSE) was applied.

ADC values were calculated by a software based on the following equation:

$$\ln S(G) - \ln S(0) - 2[\gamma \Delta^2 x G^2 \delta^2 x (\Delta - \delta/3)] \times \text{ADC}$$

where G was the amplitude of the pulse diffusion gradient, Δ the gyromagnetic ratio, γ the interval between the diffusion gradients, δ the duration of diffusion gradients, S(G) the signal strength with the pulsed diffusion gradient on, and S(0) the signal strength with the pulsed diffusion gradient off

Image Evaluation

DW images and ADC maps were transferred to a workstation. The SI of the cingulate gyrus, insula, lateral aspect of the temporal lobe (including the superior-middle temporal gyrus), the medial aspect of the occipital lobe (including the lingual gyrus), and the lateral aspect of the parietal lobe (including the supramarginal and angular gyrus), the amygdala and the hippocampus (Figure 1) were interpreted in consensus by two radiologists. We used the transverse image at the level of (i) the basal ganglia for the cingulate gyrus, insula, and lateral aspect of the temporal lobe (including the superior-middle temporal gyrus), and (ii) the medial aspect of the occipital lobe (including the lingual gyrus). At the level of centrum semiovale, we used the lateral aspect of the parietal lobe (including the supramarginal and angular gyrus). The hippocampus and amygdala were assessed at the level of red nucleus.

The SI of these regions on the DW images was classified into five grades with reference to that of frontal cortical grey matter: grade 1 = definitely less, grade 2 = slightly less, grade 3 = equal to, grade 4 = slightly greater, and grade 5 = definitely greater. The cortex of the right middle frontal gyrus was used for reference because it was constantly assessable at the levels of both the basal ganglia and centrum semiovale.

The SI and ADC value of each cortex were assessed on DW images using a region-of-interest (ROI) function on the MRI workstation. The ROI was placed according to predefined anatomical locations agreed by both observers before initiation of the study.¹ First, a ROI was placed on the $b = 0$ image obtained from DW-MRI to achieve maximum coverage while avoiding boundaries

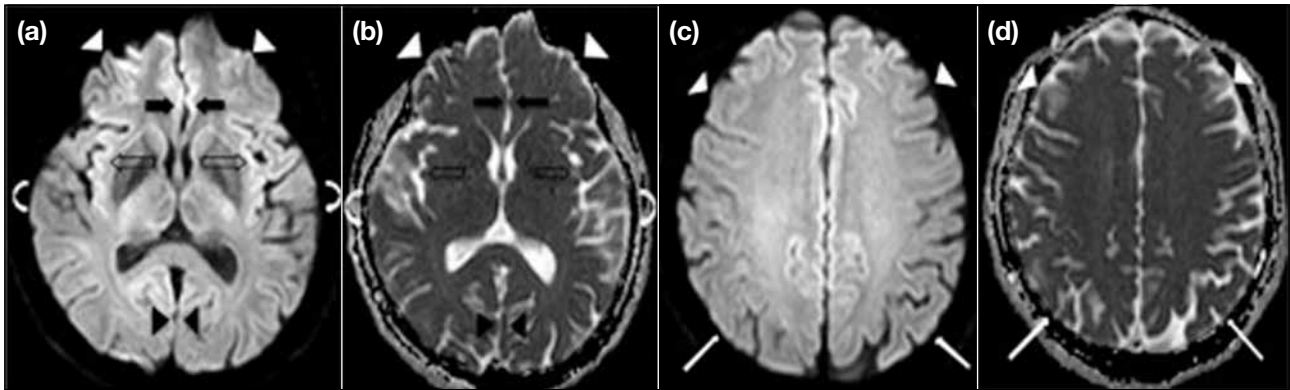


Figure 1. (a and c) Axial trace diffusion-weighted (DW) images at 3T (2800/88 TR/TE, b value of 1000 s/mm²) and (b and d) corresponding apparent diffusion coefficient (ADC) maps in a neurologically normal 49-year-old man. (a and b) Image obtained at the level of basal ganglia. The cingulate gyrus (black arrows) and insular cortex (open black arrows) show higher signal intensities relative to the middle frontal gyrus (white arrowheads). The signal intensities in the occipital cortices (black arrowheads) and temporal cortices (white curved arrows) are similar to that in the right frontal cortex. No definite signal variation is observed on ADC maps. (c and d) The DW images and ADC maps are obtained at the level of centrum semiovale. The parietal cortex (white arrows) is isointense relative to the frontal cortical grey matter (white arrowheads).

that could cause a partial volume effect from subcortical white matter, cerebrospinal fluid, and cortical veins. The smallest acceptable size of a ROI was 10 mm². The ROI was then copied onto the corresponding trace DW-MR images at b = 1000 and ADC maps, respectively (at the same anatomical position). When necessary, the observers manually adjusted the image on the basis of visual inspection. Background SI was measured in the white matter of the right frontal lobe on the same image. The contrast ratio (CR) was calculated as follows:

$$CR = (SI_{\text{cortex}} - SI_b) / (SI_{\text{cortex}} + SI_b)$$

where SI_{cortex} was the signal intensity of the cortex and SI_b the signal intensity of the background

Mean ADC values (generated automatically) for the ROIs were also obtained.

Statistical Analysis

The subjects imaged by 1.5T and 3T machines were divided into two groups. The existence of CR and ADC value differences among the anatomical locations were tested with respect to male and female subjects, and left and right hemispheres by using an analysis of variance for multiple comparisons. Once the statistically significant CR and/or ADC value differences were identified, post-hoc analyses by the Tukey's range test were performed. All statistical levels of significance were set at 5%.

RESULTS

On visual grading, increased SI at the cingulate gyrus and insula as compared to the frontal lobe cortex

was observed in most subjects. In 3T images, all 48 hemi-cerebri showed higher SI (100% grade 5) at the cingulate gyrus, while 96% (46/48) showed higher SI at the insula (grade 5: 14/48, 29%; grade 4: 32/48, 67%). Increased SI at these two regions was also observed in 1.5T images, but the effect was less pronounced (Figure 2), with 96% and 82% of hemi-cerebri carrying higher SI at the cingulate gyrus and insula, respectively. None of the cases showed lower SI on visual grading of these areas. Mildly increased SI (predominantly grade 4) at the hippocampus was also demonstrated in most subjects. The distribution of SI grades is summarised in Figure 3.

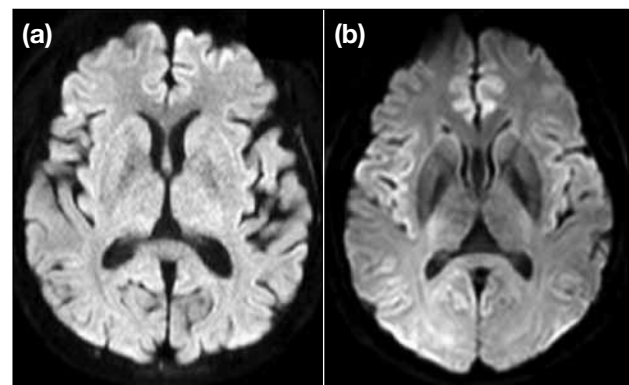


Figure 2. Diffusion-weighted images obtained at the level of basal ganglia in (a) 1.5T and (b) 3T. Higher signal intensity at the cingulate gyrus and insula is evident and more pronounced in 3T images.

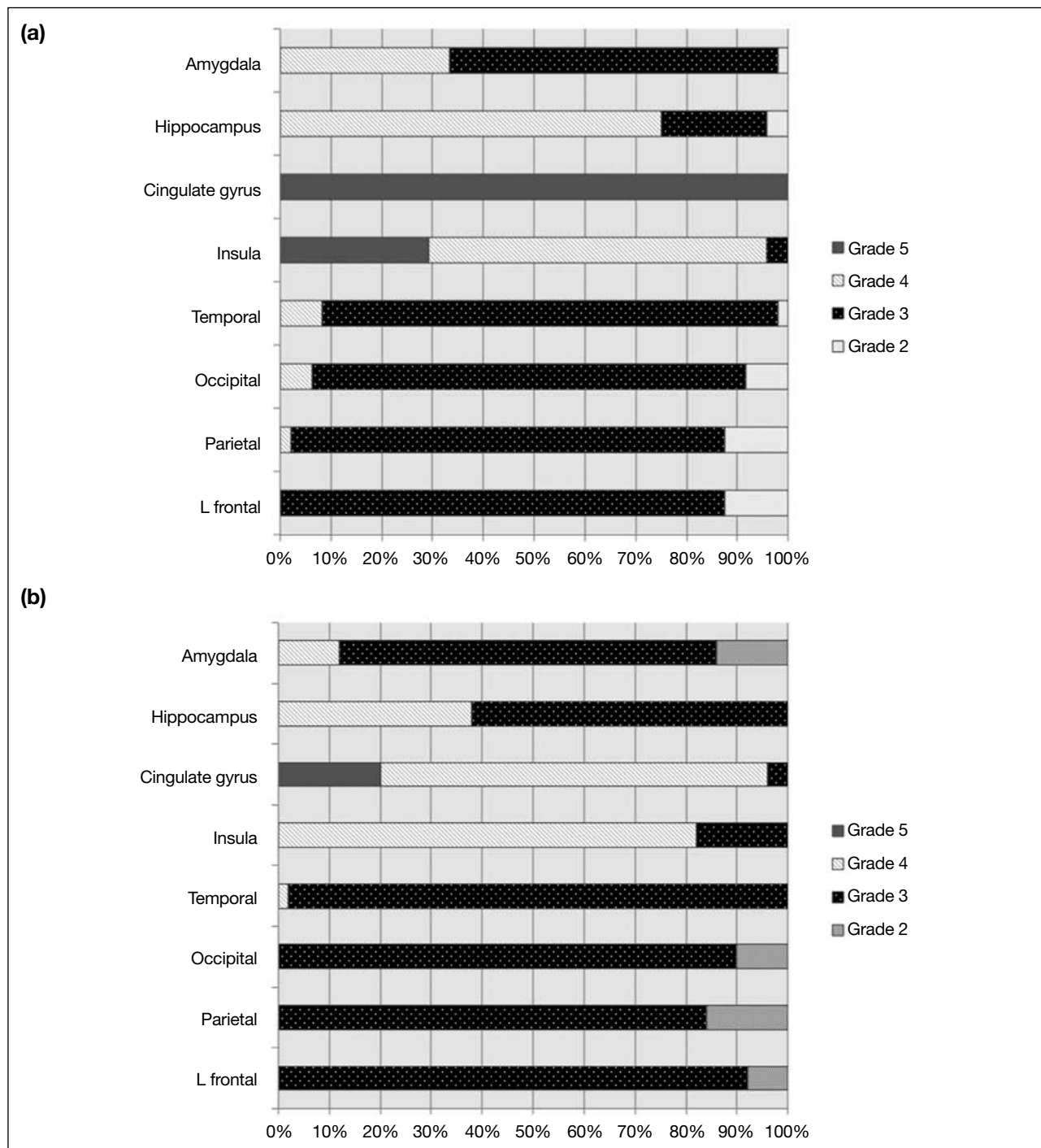


Figure 3. Distribution of signal intensity visual grades on diffusion-weighted images according to the cortical regions. Increased signal intensities at the cingulate gyrus and insula were observed in most subjects in both (a) 3T and (b) 1.5T images.

Regarding the CRs of various cortices, multiple comparisons demonstrated no statistically significant difference with respect to gender and laterality (Table 2) in most regions. However, higher SI at the right hippocampus than the left counterpart was observed in the 3T group ($p < 0.5$). There was a statistically

significant difference among cortical regions ($p < 0.0001$) in both the 1.5T and 3T groups of subjects. In the 3T group, the CRs were significantly higher in the cingulate gyrus and insula than in the other cortices ($p < 0.05$) [Figure 4]. In the 1.5T group, increased CRs were also demonstrated in both the cingulate gyrus and

Table 2. Contrast ratios (CRs) at various cortical regions according to laterality.*

Region and hemisphere	CR ($\times 10^{-2}$), mean \pm standard deviation	
	3T	1.5T
Frontal lobe cortex		
Right	11.3 \pm 6.5	13.1 \pm 5.3
Left	11.3 \pm 6.0	12.8 \pm 4.5
Parietal lobe cortex		
Right	15.2 \pm 6.8	13.4 \pm 4.0
Left	11.9 \pm 6.9	13.9 \pm 4.0
Occipital lobe cortex		
Right	17.6 \pm 7.3	15.5 \pm 4.6
Left	13.8 \pm 7.5	14.2 \pm 4.4
Temporal lobe cortex		
Right	13.1 \pm 7.5	13.7 \pm 4.0
Left	11.8 \pm 5.3	14.2 \pm 6.3
Insula		
Right	23.7 \pm 5.0	20.0 \pm 3.7
Left	22.2 \pm 4.4	21.3 \pm 3.4
Cingulate gyrus		
Right	23.3 \pm 5.0	17.3 \pm 4.2
Left	24.0 \pm 5.7	18.4 \pm 4.5
Hippocampus		
Right	23.1 \pm 6.0	18.1 \pm 4.4
Left	15.8 \pm 6.1	18.6 \pm 4.9
Amygdala		
Right	15.6 \pm 6.7	12.1 \pm 4.9
Left	13.7 \pm 6.9	14.3 \pm 4.5

* Right hippocampus shows higher CR than the left ($p < 0.05$). There was no significant difference according to laterality in other regions.

insula, though such differences did not reach statistical significance for the insular region.

In ADC maps, multiple comparisons detected no statistically significant difference between the various cortical regions in subjects imaged by both 3T and 1.5T machines.

DISCUSSION

Regional variation of SIs on the cerebral cortex is frequently observed in neurologically normal subjects. The depiction of such heterogeneity becomes more obvious with high-strength 3T-MRI than with 1.5T machines. Several reports suggested that there are both cortical areas of signal heterogeneity on DWI and differences in the ADCs between grey and white matter. However, systematic studies of such differences in various areas of cortical grey matter are scarce. The recognition of normal variations in the SI of different areas of cortical grey matter on DWI is important, so as to avoid erroneous diagnoses of neurological diseases, particularly those entailing cortical pathology.

Our results confirm the previously reported observations by Asao et al¹⁹ and show higher SI in the cingulate gyrus and insula than in other cortical areas. Also, we quantitatively demonstrated that there are no ADC value differences among various regions, which have not been studied before. The SI on DW image is affected by several factors, namely: tissue T2 characteristics, ADC, b values, spin attenuation, and TE.²⁰ Since the b value and TE were constant in our study, only T2 characteristics, ADC, and spin attenuation could have affected our results. The ADC of biological tissue reflects the motion of protons within the cellular structures using an average of three orthogonal directions. Based on our results, there was no significant difference in ADC values among various cortical regions. This may imply that the inhomogeneity of signals on DW images is not related to diffusion within tissues. Variation of T2 in brain tissue has been described, and can be attributed to factors such as water content,²¹ cytoarchitecture, and iron contents.²² Whittall et al²¹ used T2 decay curves, and Georgiades et al²³ investigated T2 relaxation; both reported significantly higher signals in the cingulate gyrus and insular cortex than in other cortical grey matter structures. Hirai et al¹⁶ reported that the SI of the cingulate gyrus and insular cortex on turbo FLAIR images was higher (based on contrast-to-noise measurements). Because DW images are inherently T2-weighted, changes in tissue T2 can influence the appearance of DW images independent of diffusion within tissues.²⁰ Thus, the increased SI in the cingulate gyrus and insula that we observed on DW images is actually attributable to a T2 shine-through effect.

Based on differences in lamination, the cerebral cortex can be classified into at least two major groups: a six-layered neocortex that contributes most of the cerebral cortex, and an allocortex with less than six layers (varying in number), that contributes the olfactory cortex, amygdala, and the hippocampal formation. The periallocortex comprises the interface of these two cortices, including the cingulate gyrus, parahippocampal gyri and insula.²⁴⁻²⁶ Each of the different cortical layers contains a characteristic distribution of neuronal cell types and connections with other cortical and subcortical regions. In our study, the SIs of the periallocortex were higher than that of the neocortex on DW images, which might correlate with its cellular composition induced by cortical development. The use of high-field MRI further accentuates this difference. High field strength (3T) MR system is considered to offer double the signal-to-noise

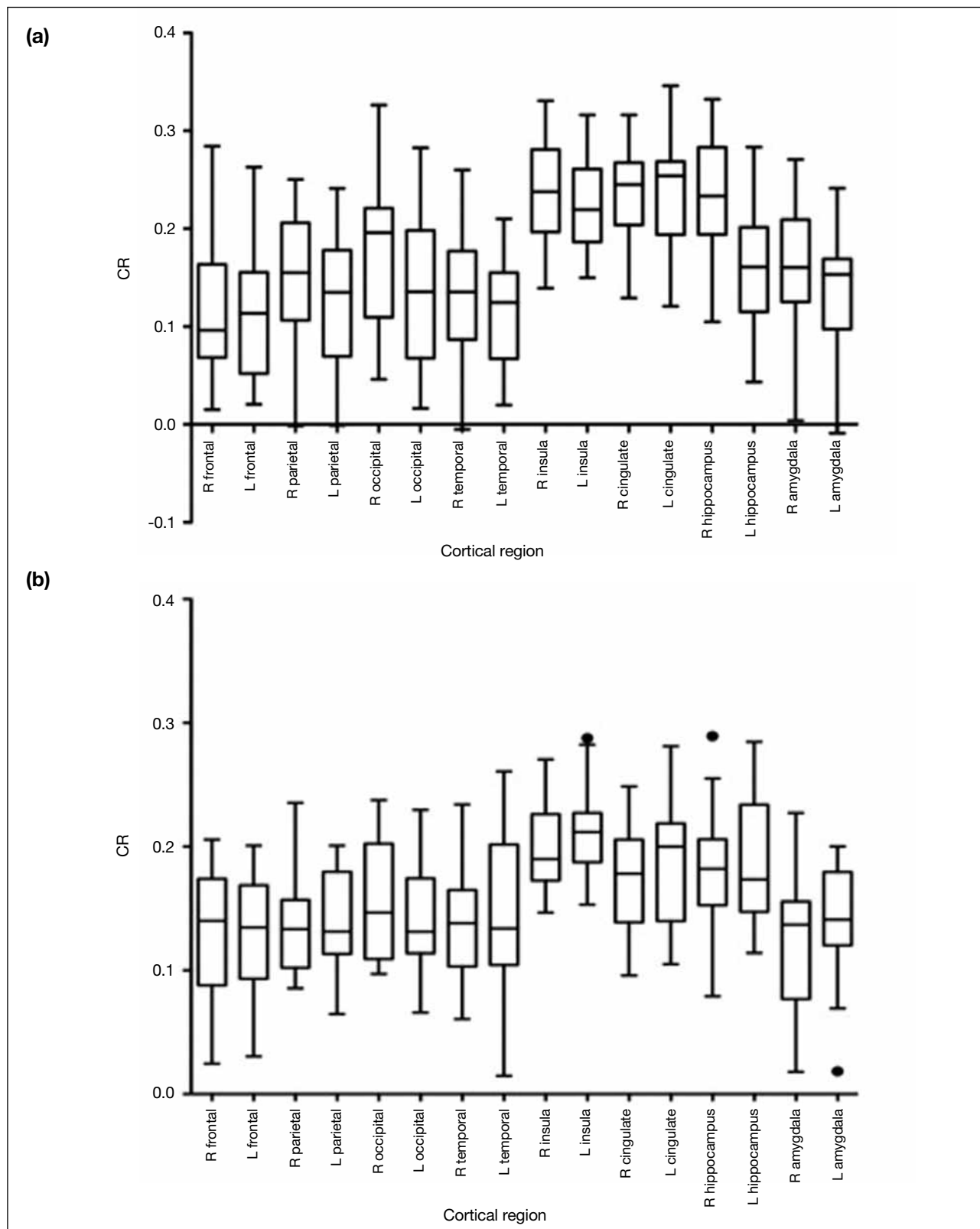


Figure 4. Box-and-Whisker plots show mean contrast ratios (CRs) measured in each cortex from 98 cerebral hemispheres with respect to laterality at (a) 3T and (b) 1.5T. The CR was significantly higher in the cingulate gyrus and insula than the other cortices ($p < 0.05$) in 3T images. Though a similar pattern was demonstrated with 1.5T images, it did not attain statistical significance. No significant difference in CRs was demonstrated among other cortices. The horizontal lines within the boxes represent the medians, the lower and upper bounds of the boxes represent the 25th and 75th percentiles, and the I bars represent the 5th and 95th percentiles. The circles indicate outliers. Abbreviations: L = left; R = right.

ratio compared with that offered by the 1.5T reference standard.²⁷ This potential benefit is not straightforward, but complicated by the fact that high magnetic field strength will degrade DW-MR images, because of stronger susceptibility effects and image blurring. Incorporating the techniques of parallel imaging into our routine DW imaging protocol improved image quality,²⁸ so we could demonstrate cortical heterogeneity on DW images more easily with 3T than 1.5T machines.

Among the isocortical areas, Yoshiura et al¹⁵ observed a decrease in SI in the primary auditory cortex on T2-weighted MR images. Hirai et al¹⁶ also described markedly higher SI at the limbic lobe and a slightly increase at the frontal cortex on FLAIR images. In our study, we observed relatively higher SIs on the hippocampus, particularly on the right side. Anyhow, such difference did not reach statistically significant levels. In our study, as the limbic system is best delineated on coronal images, using axial sections may limit the assessment and hence not be comparable with previous results.

Cortical diffusion abnormalities can be demonstrated in a spectrum of diseases,²⁹ including infarction, hypoxic ischaemic encephalopathy, encephalitis, CJD, mitochondrial cytopathies and post-ictal states. In the early stages of CJD and cortical infarcts, DW images may be the only sequence to depict the abnormality while conventional T1-weighted and T2-weighted MR images remain normal³⁰⁻³³ (Figure 5). Therefore, knowledge of normal patterns in the cerebral cortex is crucial to avoid misdiagnoses. Our study revealed

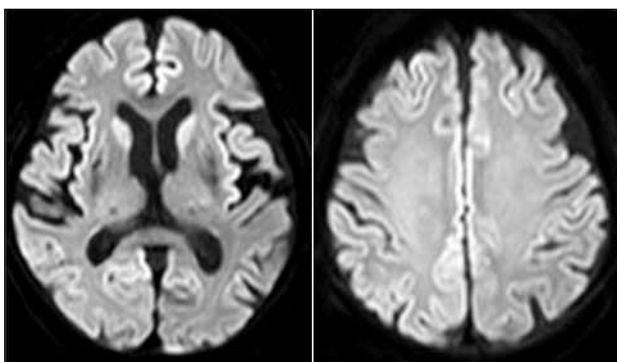


Figure 5. Creutzfeldt-Jakob disease in a 78-year-old female; 3T magnetic resonance diffusion-weighted images show symmetrical high signal at bilateral cerebral cortices, including cingulate gyrus and insular cortices. However in this case, abnormal signals extend to frontal, parietal cortices and caudate heads on both sides, thus differentiating this pathological condition from physiological change.

the presence of a regional high signal at the cingulate gyrus and insula on DW images from healthy subjects, such heterogeneity being present irrespective of age and gender. Thus, radiologists should be aware of physiologically high SI in these regions on DW images. When in doubt, scrutinising the ADC map for any corresponding restricted diffusion change might be helpful.

One limitation of this study was the questionable reliability of using the frontal white matter as the background tissue for quantitative analysis, particularly with respect to the effect of age-related increases in iron contents in the white matter. It has been reported that the iron contents of the frontal lobe remains nearly stable after age 30 years.³⁴ Because most of the subjects in our study were older than 30 years, we believe that the effect of iron content was trivial and that frontal white matter could be reasonably used as a reference background. The use of frontal white matter as an internal reference might also be challenged as subject to artefacts near the skull base and frontal sinuses, due to the effect of bone inhomogeneity and susceptibility variations causing geometric distortion at interfaces between soft tissue and bone or air. However, this problem was insignificant in our study as the frontal white matter was chosen at the level of the basal ganglia and centrum semiovale, in which such artefacts are negligible. A second limitation was that since not all cerebral cortices are located on the same section, it might be difficult to directly compare the SI differences visually. To circumvent this problem of visual grading of various cerebral cortices, we standardised the predefined anatomical regions on two sections (at the centrum semiovale and basal ganglia). Also, the use of frontal cortex as a reference seems to be suitable as it can be visualised on both sections. We believe that our visual grades correlated with cortical SI as it showed good agreement with our quantitative results. A third limitation was imposed by partial volume effect. We used images with a section thickness of a 5-mm and a 1-mm intersection gap. Partial volume effects may not be negligible when evaluating cortical SI. Brain atrophy, especially cortical atrophy, associated with ageing might affect cortical SI. A fourth limitation was that we employed an imaging protocol that corrected background noise to zero, as in our routine practice. In such setting, the measured background noise did not represent random noise anymore. Therefore, we could not calculate the contrast-to-noise ratio. Instead, we measured the CR that reflects the signal contrast

in the cerebral cortex with respect to the background. Direct comparison with other published studies is hence impossible.

CONCLUSION

We evaluated the normal appearance of the cerebral cortex on DW-MR images. High SI in the insula and cingulate gyrus is frequently encountered in neurologically healthy subjects regardless of patient age, gender, and laterality. Absence of ADC map differences signifies that these findings are not related to restricted diffusion, but are caused by T2 shine-through effect. 3T MRI accentuates the depiction of physiological cortical heterogeneity on DWI. It is important to recognise normal heterogeneity of cortices in order to avoid erroneous diagnoses of pathological conditions. We believe that the results of this preliminary study will lead to further large-scale randomised trials with the aim of developing clinically useful standards in this regard.

REFERENCES

- Sorensen AG, Buonanno FS, Gonzalez RG, Schwamm LH, Lev MH, Huang-Hellinger FR, et al. Hyperacute stroke: evaluation with combined multisection diffusion-weighted and hemodynamically weighted echo-planar MR imaging. *Radiology*. 1996;199:391-401.
- Marks MP, de Crespigny A, Lentz D, Enzmann DR, Albers GW, Moseley ME. Acute and chronic stroke: navigated spin-echo diffusion-weighted MR imaging. *Radiology*. 1996;199:403-8.
- Lövblad KO, Laubach HJ, Baird AE, Curtin F, Schlaug G, Edelman RR, et al. Clinical experience with diffusion-weighted MR in patients with acute stroke. *AJNR Am J Neuroradiol*. 1991;12:1061-6.
- Ukisu R, Kushihashi T, Tanaka E, Baba M, Usui N, Fujisawa H, et al. Diffusion-weighted MR imaging of early-stage Creutzfeldt-Jakob disease: typical and atypical manifestations. *Radiographics*. 2006;26 Suppl 1:S191-204. [crossref](#)
- Heiner L, Demaerel P. Diffusion-weighted MR imaging findings in a patient with herpes simplex encephalitis. *Eur J Radiol*. 2003;45:195-8. [crossref](#)
- Küker W, Nägele T, Schmidt F, Heckl S, Herrlinger U. Diffusion-weighted MRI in herpes simplex encephalitis: a report of three cases. *Neuroradiology*. 2004;46:122-5. [crossref](#)
- Donaire A, Carreno M, Gómez B, Fossas P, Bargalló N, Agudo R, et al. Cortical laminar necrosis related to prolonged focal status epilepticus. *J Neurol Neurosurg Psychiatry*. 2006;77:104-6. [crossref](#)
- Senn P, Lövblad KO, Zutter D, Bassetti C, Zeller O, Donati F, et al. Changes on diffusion-weighted MRI with focal motor status epilepticus: case report. *Neuroradiology*. 2003;45:246-9.
- Cole AJ. Status epilepticus and periictal imaging. *Epilepsia*. 2004;45 Suppl 4:72-7. [crossref](#)
- Ay H, Buonanno FS, Schaefer PW, Le DA, Wang B, Gonzalez RG, et al. Posterior leukoencephalopathy without severe hypertension: utility of diffusion-weighted MRI. *Neurology*. 1998;51:1369-76. [crossref](#)
- Torack RM, Alcalá H, Gado M, Buron R. Correlative assay of computerized cranial tomography (CCT) water content and specific gravity in normal and pathological postmortem brain. *J Neuropath Exp Neurol*. 1976;35:385-92. [crossref](#)
- Vymazal J, Brooks RA, Patronas N, Hajek M, Bulte JW, Di Chiro GD. Magnetic resonance imaging of brain iron in health and disease. *J Neurol Sci*. 1995;134 Suppl:19-26. [crossref](#)
- van Zijl PC, Eleff SM, Ulatowski JA, Oja JM, Uluğ AM, Traystman RJ, et al. Quantitative assessment of blood flow, blood volume, and blood oxygenation effects in functional magnetic resonance imaging. *Nat Med*. 1998;4:159-67. [crossref](#)
- Oja JM, Gillen JS, Kauppinen RA, Kraut M, van Zijl PC. Determination of oxygen extraction ratios by magnetic resonance imaging. *J Cereb Blood Flow Metab*. 1999;19:1289-95. [crossref](#)
- Yoshiura T, Higano S, Rubio A, Shrier DA, Kwok WE, Iwanaga S, et al. Heschl and superior temporal gyri: low signal intensity of the cortex on T2-weighted MR images of normal brain. *Radiology*. 2000;214:217-21.
- Hirai T, Korogi Y, Yoshizumi K, Shigematsu Y, Sugahara T, Takahashi M. Limbic lobe of the human brain: evaluation with turbo fluid-attenuated inversion-recovery MR imaging. *Radiology*. 2000;215:470-5.
- DeLano MC, Cooper TG, Siebert JE, Potchen MJ, Kuppusamy K. High-b-value diffusion-weighted MR imaging of adult brain: image contrast and apparent diffusion coefficient map features. *AJNR Am J Neuroradiol*. 2000;21:1830-6.
- Young GS, Geschwind MD, Fischbein NJ, Martindale JL, Henry RG, Liu S, et al. Diffusion-weighted and fluid-attenuated inversion recovery imaging in Creutzfeldt-Jakob disease: high sensitivity and specificity for diagnosis. *AJNR Am J Neuroradiol*. 2005;26:1551-62.
- Asao C, Hirai T, Yoshimatsu S, Matsukawa T, Imuta M, Sagara K, et al. Human cerebral cortices: signal variation on diffusion-weighted MR imaging. *Neuroradiology*. 2008;50:205-11. [crossref](#)
- Hiwatashi A, Kinoshita T, Moritani T, Wang HZ, Shrier DA, Numaguchi Y, et al. Hypointensity on diffusion-weighted MRI of the brain related to T2 shortening and susceptibility effects. *AJR Am J Roentgenol*. 2003;181:1705-9. [crossref](#)
- Whittall KP, MacKay AL, Graeb DA, Nugent RA, Li DK, Paty DW. In vivo measurement of T2 distributions and water contents in normal human brain. *Magn Reson Med*. 1997;37:34-43. [crossref](#)
- Vymazal J, Hajek M, Patronas N, Giedd JN, Bulte JW, Baumgarner C, et al. The quantitative relation between T1-weighted and T2-weighted MRI of normal gray matter and iron concentration. *J Magn Reson Imaging*. 1995;5:554-60. [crossref](#)
- Georgiades CS, Itoh R, Golay X, van Zijl PC, Melhem ER. MR imaging of the human brain at 1.5 T: regional variations in transverse relaxation rates in the cerebral cortex. *AJNR Am J Neuroradiol*. 2001;22:1732-7.
- Ribas GC. The cerebral sulci and gyri. *Neurosurg Focus*. 2010;28:E2. [crossref](#)
- Samat HB, Netsky MG. Evolution of the nervous system. 2nd ed. New York: Oxford University Press; 1981.
- Chronister RB, White LE. Fiber architecture of the hippocampal formation: anatomy, projections, and structural significance. In: Isaacson RL, Pribram KH, editors. *The hippocampus, vol 1, structure and development*. New York: Plenum Press; 1975. p 9-39.
- Willinek WA, Schild HH. Clinical advantages of 3.0 T MRI over 1.5 T. *Eur J Radiol*. 2007;65:2-14. [crossref](#)
- Kuhl CK, Gieseke JM, von Falkenhausen, Textor J, Gernert S, Sonntag C, et al. Sensitivity encoding for diffusion-weighted MR imaging at 3.0 T: intraindividual comparative study. *Radiology*. 2005;234:517-26. [crossref](#)
- Sheerin F, Pretorius PM, Briley D, Meagher T. Differential diagnosis of restricted diffusion confined to the cerebral cortex. *Clin Radiol*. 2008;63:1245-53. [crossref](#)

30. González RG, Schaefer PW, Buonanno FS, Schwamm LH, Budzik RF, Rordorf G, et al. Diffusion-weighted MR imaging: Diagnostic accuracy in patients imaged within 6 hours of stroke symptom onset. *Radiology*. 1999;210:155-62.
31. Ukisu R, Kushihashi T, Kitano T, Fujisawa H, Takenaka H, Ohgiya Y, et al. Serial diffusion-weighted MRI of Creutzfeldt-Jakob disease. *AJR Am J Roentgenol*. 2005;184:560-6. [cross ref](#)
32. Murata T, Shiga Y, Higano S, Takahashi S, Mugikura S. Conspicuity and evolution of lesions in Creutzfeldt-Jakob disease at diffusion-weighted imaging. *AJNR Am J Neuroradiol*. 2002;23:1164-72.
33. Finkenstaedt M, Szudra A, Zerr I, Poser S, Hise JH, Stoebner JM. MR imaging of Creutzfeldt-Jakob disease. *Radiology*. 1996;199:793-8.
34. Hallgren B, Sourander P. The effect of age on the non-haemin iron in the human brain. *J Neurochem*. 1958;3:41-51. [cross ref](#)

Corrigendum

“Radiological Features of Osteogenesis Imperfecta Type V: a Report of Two Cases” (March 2012;15:36-40). On page 36, the authorship list should have read:

PKT Hui¹, JYL Tung², MKT To³, W Chow³, WWM Lam¹, MT Chau¹

許其達、童月玲、杜啟峻、周宏、林慧文、周明德

¹Department of Radiology, and ²Department of Paediatrics and Adolescent Medicine, Queen Mary Hospital, The University of Hong Kong, Pokfulam Road, Hong Kong; ³Department of Orthopaedics and Traumatology, The Duchess of Kent Children's Hospital, Sandy Bay, Hong Kong